



## Polymer Communication

# The crystallization characterization of bulk syndiotactic polystyrene sample: immediate evidence from IR spectroscopy

Shoei-Chin Wu, Feng-Chih Chang\*

*Institute of Applied Chemistry, National Chiao-Tung University, Hsinchu 30050, Taiwan, ROC*

Received 2 April 2003; received in revised form 20 November 2003; accepted 29 November 2003

**Abstract**

The crystallization characterization of *bulk* syndiotactic polystyrene (*s*-PS) sample is thoroughly studied using the Fourier transform infrared spectroscopy (FTIR). The WAXD is further used to identify the *s*-PS crystal formation to confirm the specific absorbance in FTIR spectra. Both melt and cold-crystallization behavior are quantitatively determined using FTIR spectra ranging from 870 to 820  $\text{cm}^{-1}$  at 264 °C. Fitting curves to IR spectra provides direct evidence of bulk *s*-PS crystallization behavior in quantification. The melt-crystallization process yields the  $\beta$ -form only; while the cold-crystallization process yields both the  $\alpha$  and the  $\beta$ -form crystal in bulk *s*-PS sample. The  $\beta$ -form crystal is generated from the phase-transformation of the  $\alpha$ -form crystal by cold-crystallization process, the  $\alpha$ -form crystal is the initial phase. The activity energy of the  $\alpha$ -form formation is lower than that of the  $\beta$ -form, suggesting that the  $\alpha$ -form crystal is kinetically favorable while the  $\beta$ -form crystal is thermodynamically favorable.

© 2003 Published by Elsevier Ltd.

**Keywords:** Syndiotactic polystyrene; Fourier transform infrared spectroscopy; Polymer crystallization**1. Introduction**

Many studies have reported the following complicated phenomena with reference to using the differential scanning calorimetry (DSC) trace and WAXD spectra [1–6]: the development of  $\alpha$  or  $\beta$ -form crystals in the *bulk s*-PS sample, favored either kinetically or thermodynamically during the crystallization; the formation of the pure  $\alpha$  or  $\beta$ -form, or of the mixed ( $\alpha + \beta$ ) form of a crystal of *s*-PS depends upon the condition of crystallization. When the cooling rate is sufficiently high, only the  $\alpha$ -form can be crystallized; the  $\beta$ -form is obtained when the cooling rate is lower. The re-crystallization occurred during DSC heating scan that would complicate the characterization of the crystallization in bulk *s*-PS sample. The X-ray diffraction patterns can identify clearly the *s*-PS crystal form without doubt, however, its sensitivity hinder the convenience of crystallinity calculation. It is apparently that the quantitative determination and immediate evidence are lacking, furthermore, particular crystal forms in bulk *s*-PS have not yet to be quantitatively understood.

FTIR has proven to be a powerful tool in polymer science for several years [1,7–12]. It is used to elucidate crystal-

linity, structure, kinetics, thermodynamics and other properties. It complements other techniques in providing detailed information in a nondestructive and fast way. For example, the change of crystallinity and crystal conformation can be characterized by identifying through the identification of IR spectral features in terms of intensity, bandwidth, and position.

In our previous study [11,12,14], the crystallization of *thin* film *s*-PS had been studied and quantified using FTIR spectra. In this study, an FTIR spectrum is used to evidence and quantify immediately the crystallization behavior of pure bulk *s*-PS sample. This work has two aims: (1) to characterize evidence immediately the bulk *s*-PS crystallization characterization; and (2) more importantly, to discuss the phase-transformation between the  $\alpha$  and  $\beta$ -form crystal in a bulk *s*-PS sample during the cold-crystallization heating treatment process.

**2. Experimental section****2.1. Materials**

The *s*-PS was kindly donated by the Industrial Technology Research Institute (ITRI, HsinChu, Taiwan) and was used without further purification. The stereoregularity of the

\* Corresponding author. Tel.: +886-3-5727077; fax: +886-3-5719507.  
E-mail address: [changfc@mail.ntcu.edu.tw](mailto:changfc@mail.ntcu.edu.tw) (F.C. Chang), [muddaxac.ac87g@ntcu.edu.tw](mailto:muddaxac.ac87g@ntcu.edu.tw) (F.C. Chang).

syndiotactic polystyrene with  $M_n = 56,000$  g/mol was  $[\text{rr}] = 99\%$  from identified by the solution  $^{13}\text{C}$  NMR spectrum. The bulk s-PS sample was obtained by solution casting on a KBr disk with a thickness more than  $100\ \mu\text{m}$ , which pretreated at  $320\ ^\circ\text{C}$  for 20 min to eliminate the residual crystal memory. It was then quenched in liquid nitrogen to obtain the amorphous (crystal-free) bulk s-PS as the starting material.

## 2.2. Characterizations

The formation of thin film s-PS is description in our previous report [11]. The bulk s-PS sample is obtained from ITRI without any procedure. In DSC tracing, the s-PS samples were heated at a scanning rate of  $10\ ^\circ\text{C}/\text{min}$  from  $30\ ^\circ\text{C}$ . Isothermal cold and melt-crystallizations of samples were performed with various time intervals in an environmental chamber with a temperature programmable controller within an accuracy of  $\pm 0.1\ ^\circ\text{C}$ . For cold-crystallization, the quenched s-PS sample was placed directly into the chamber at  $264\ ^\circ\text{C}$ . For the melt-crystallization, the s-PS sample was heated to  $320\ ^\circ\text{C}$  for 5 min and quickly cooled ( $-100\ ^\circ\text{C}/\text{min}$ ) to  $264\ ^\circ\text{C}$ . All samples were prepared under a continuous nitrogen flow to minimize the oxidation or degradation of the sample. For WAXD experiments, A Siemens D5000 1.2 kW tube X-ray generator (Cu K $\alpha$  radiation) with a diffractometer was used for WAXD powder experiments. The scanning of  $0.05^\circ$  for 3 s. The diffraction peak positions and widths observed from WAXD were carefully calibrated with silicon crystals with know crystal size. The crystal form and crystallinity of the s-PS were characterized by infrared spectroscopy (Nicolet AVATAR 320 FTIR spectrometer, USA) with a resolution of  $1.0\ \text{cm}^{-1}$  at  $30\ ^\circ\text{C}$ , ranging from  $870$  to  $820\ \text{cm}^{-1}$ . The frequency scale was internally calibrated using a He–Ne laser, and 256 scans were single-averaged to reduce the noise. FTIR spectral features were resolved using curving-fitting analysis to quantify the area and positions. The peaks are assumed to be Gaussian with a linear baseline. It was found that the standard error for the measured area used in this curve fitting analysis was approximately 2–3%. The absolute crystallinity of  $\alpha$  and  $\beta$ -forms of s-PS can be calculated from the following equations [14]:

$$C_\alpha = \frac{A_{851}/a_\alpha}{A_{841} + A_{851}/a_\alpha + A_{858}/a_\beta} \times 100\% \quad (1)$$

$$C_\beta = \frac{A_{858}/a_\beta}{A_{841} + A_{851}/a_\alpha + A_{858}/a_\beta} \times 100\% \quad (2)$$

where  $C_\alpha$  and  $C_\beta$  represent the crystallinities of the  $\alpha$  and  $\beta$ -forms, respectively;  $A_{841}$ ,  $A_{851}$  and  $A_{858}$  are the area fractions of amorphous,  $\alpha$  and  $\beta$ -forms, as obtained by the absorbance ranging from  $870$  to  $820\ \text{cm}^{-1}$ . The conversion coefficients  $a_\alpha$  and  $a_\beta$  ( $0.178$  and  $0.272$  obtained from a previous studies) are the ratios of absorptive coefficients of

$A_{851}/A_{841}$  and  $A_{858}/A_{841}$  for  $\alpha$  and  $\beta$ -form crystal absorbance, respectively.

## 3. Results and discussion

### 3.1. DSC traces

Fig. 1 shows the DSC  $10\ ^\circ\text{C}/\text{min}$  traces of a quenched bulk s-PS sample (start material) with amorphous phase since total transparency was observed. Only one asymmetric endothermic peak at  $\sim 267\ ^\circ\text{C}$  corresponds to the  $\alpha$ -form. Therefore, the amorphous s-PS will mostly crystallized to form the  $\alpha$ -form crystal during DSC heating scanning ( $10\ ^\circ\text{C}/\text{min}$ ). The further evidence will be further described in Fig. 3a.

Fig. 2a–d shows the DSC  $10\ ^\circ\text{C}/\text{min}$  heating rate of bulk s-PS which cold-crystallized at  $264\ ^\circ\text{C}$  for 5, 15, 30 and 60 min, respectively. Fig. 2a–c shows two asymmetric peaks: a higher temperature melting peak around  $\sim 270\ ^\circ\text{C}$  corresponding to the  $\alpha$ -form crystal; and a lower peak around  $\sim 260\ ^\circ\text{C}$  corresponding to the  $\beta$ -form crystal [6]. The new  $\beta$ -form crystal asymmetric peak implies that the  $\beta$ -form crystal was formed during the DSC heating scanning in the cold-crystallized s-PS bulk sample. The  $\beta$ -form peak shifts gradually to a higher temperature and the  $\beta/\alpha$  area ratio also increases gradually with the cold-crystallization time intervals increased. The  $\alpha$  and  $\beta$ -forms of crystals are found to together as shown in Fig. 2d when s-PS is cold-crystallized for 60 min. The cold-crystallization of s-PS is inferred to dictate not only to the  $\beta/\alpha$  area ratio but also to the perfection of  $\beta$ -form crystal. This result supports the fact that the  $\beta$ -form crystal is thermodynamically favored [1,2]. Inferred from Figs. 1 and 2, both  $\alpha$  and  $\beta$ -form crystals may be formed during cold-crystallization in bulk s-PS sample. The crystallization behavior of bulk s-PS is not fully elucidated and quantified by the observation of DSC heating

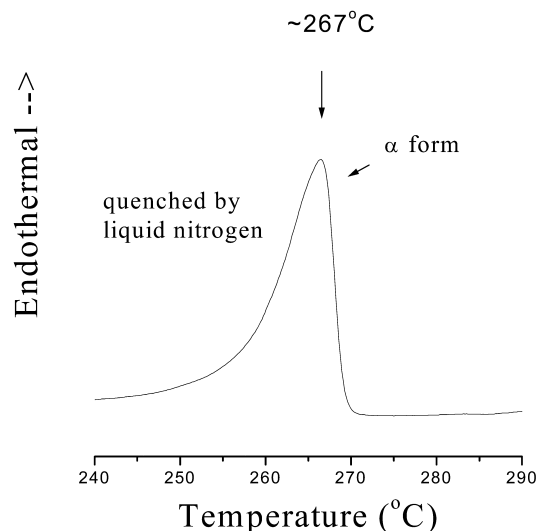


Fig. 1. DSC thermograms of quenched bulk s-PS sample.

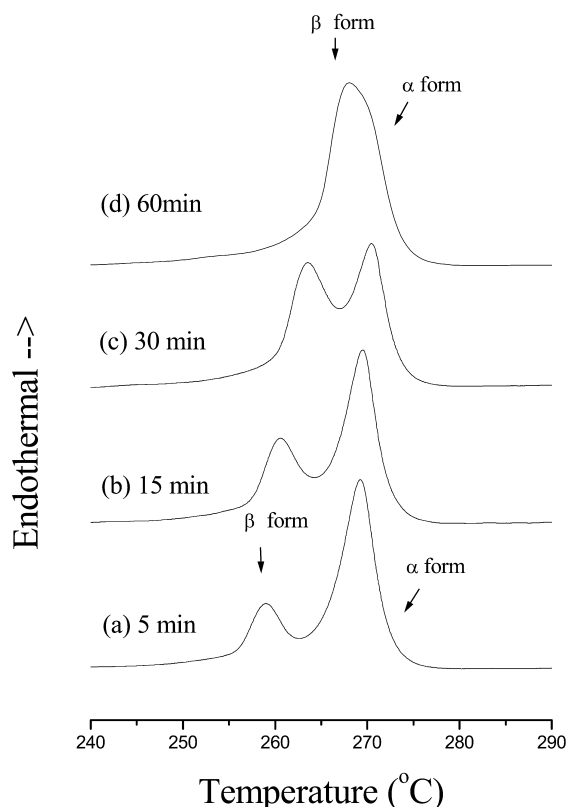


Fig. 2. DSC heating scan of bulk s-PS which melt-crystallized at 264 °C for (2a) 5 min; (2b) 15 min; (2c) 30 min; (2d) 60 min.

scanning procedure due to the re-crystallization would occur. The exit section considers the immediate evidence of bulk s-PS crystallization behavior in the form of FTIR spectra.

### 3.2. WAXD spectrum

The melt-crystallized and cold-crystallized thin film

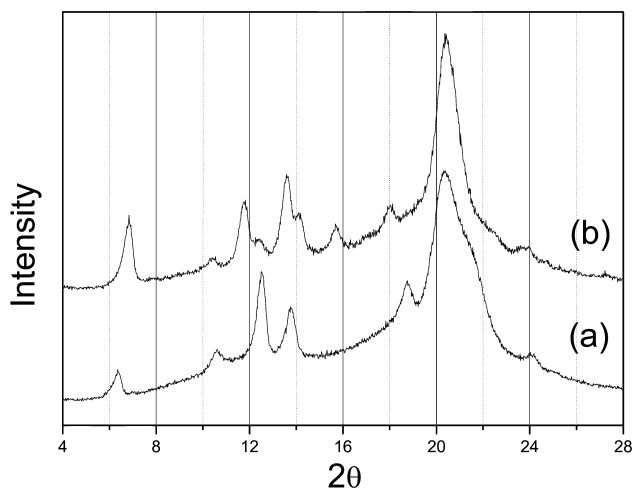


Fig. 3. WAXD diffraction patterns of (3a) melt-crystallized; (3b) cold-crystallized thin film s-PS sample (the intensity have been normalized).

samples were thoroughly examined using WAXD to identify their corresponding crystal structures, as shown in Fig. 3. (i.e. single  $\alpha$  form, single  $\beta$  form and amorphous). There is no specific characteristic diffraction peak shows in WAXD pattern in starting material sample, as shown in Fig. 3a. It is apparent that the starting material is amorphous totally, means that the endothermic peak in Fig. 1 is resulted from recrystallization in DSC heating process.

The characteristic diffraction peaks of  $\beta$  form (i.e.  $2\theta = 6.2, 12.3, 18.6, 20.2,$  and  $21.3^\circ$ ) in WAXD pattern were clearly observed in melt-crystallized thin film sample, as shown in Fig. 3b. Only single  $\beta$  form was formed in melt-crystallized thin film sample. The cold-crystallized thin film sample only exhibits the entity of the single  $\alpha$  form as shown in Fig. 3c (characteristic peaks at  $2\theta = 6.7, 11.7, 14.0, 15.6,$  and  $20.3^\circ$ ). These results suggest that isolated  $\alpha$  form and  $\beta$  form crystals can be obtained by cold and melt-crystallization in thin film sample, respectively.

### 3.3. IR spectrum

Table 1 summarizes the specific absorbance of s-PS in the IR spectrum ranging from  $870$  to  $820\text{ cm}^{-1}$  [11–14]. The specific absorbance of the amorphous phase appears at  $841\text{ cm}^{-1}$ . Specific absorbance of the  $\alpha$ -form crystal occurs at  $851\text{ cm}^{-1}$  (shifted from  $841\text{ cm}^{-1}$ ), while that of the  $\beta$ -form crystal occurs at  $858\text{ cm}^{-1}$  (shifted from  $841\text{ cm}^{-1}$ ). Fig. 4a and b shows the IR spectra of melt and cold-crystallized thin film s-PS sample, respectively, from  $870$  to  $820\text{ cm}^{-1}$ , respectively. There are two apparent absorbances ( $858$  and  $840\text{ cm}^{-1}$ ) correspond to the  $\beta$ -form and amorphous phase in Fig. 4a; and two apparent absorbances ( $851$  and  $840\text{ cm}^{-1}$ ) correspond to the  $\alpha$ -form crystal and amorphous phase in Fig. 4b. The specific absorbance of FTIR spectra rather matches the result of WAXD, and previous study [11–14].

Fig. 5a and b shows the IR spectra of a quenched and cold-crystallized 2 min bulk s-PS sample, respectively, from  $870$  to  $820\text{ cm}^{-1}$ . Only one absorbance ( $841\text{ cm}^{-1}$ ) is observed to correspond to the amorphous phase in Fig. 5a; and the absorbance corresponding to both  $\alpha$  and  $\beta$ -form crystal ( $851$  and  $858\text{ cm}^{-1}$ ) were absent due to a lack of crystallization. There are three apparent absorbances correspond to the  $\alpha$ -form, the  $\beta$ -form and the amorphous phase in Fig. 5b are associated with cold-crystallization.

Table 1

The specific characterized absorbance of s-PS in IR spectrum ranging from  $870$  to  $820\text{ cm}^{-1}$

Morphology	Position of absorbance ( $\text{cm}^{-1}$ )
Amorphous phase	841 (m)
$\alpha$ -Form crystal	851(w)
$\beta$ -Form crystal	858(w)

Note: 'm', and 'w' represents for the 'middle' and 'weak' absorbances in IR spectrum, respectively.

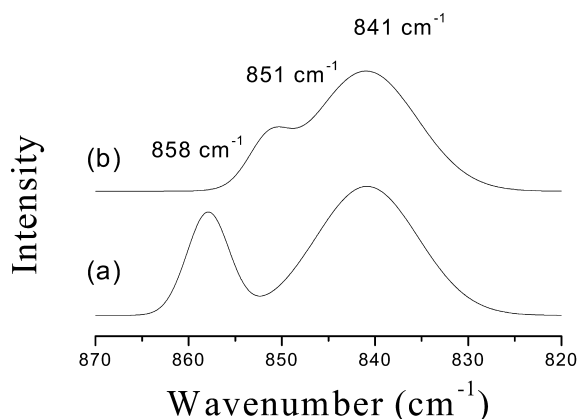


Fig. 4. FTIR spectra of the thin film s-PS sample ranging from 870 to 820  $\text{cm}^{-1}$  (4a) melt-crystallized sample; (4b) cold-crystallized sample.

### 3.4. Characterization of melt-crystallization

Fig. 6a–e presents the IR spectra of the bulk s-PS sample ranging from 870 to 820  $\text{cm}^{-1}$  under melt-crystallization following 2, 5, 10, 15, and 30 min, respectively. The curve-fitting analysis of the FTIR spectral feature reveals the presence of two distinct components— $\beta$ -form crystal absorbance (858  $\text{cm}^{-1}$ ) and amorphous absorbance (841  $\text{cm}^{-1}$ ), as shown in Fig. 6(i) and (ii), which are obtained by fitting curves to Fig. 5a as an example. Table 2 shows the results of curve-fitting and crystallinity calculated from Eqs. (1) and (2). The absorbance corresponding to  $\alpha$ -form crystal does not show in Fig. 6, implying that only the  $\beta$ -form is crystallized through melt-crystallization, but no  $\alpha$ -form crystal is formed. The area of the  $\beta$ -form crystal absorbance and the fraction of crystallinity increases with increasing the melt-crystallization time intervals, as shown in Fig. 6 and Table 2. The absolute crystallinity is 0.31 when the melt-crystallization time interval is 2 min; and reaches  $\sim 0.55$

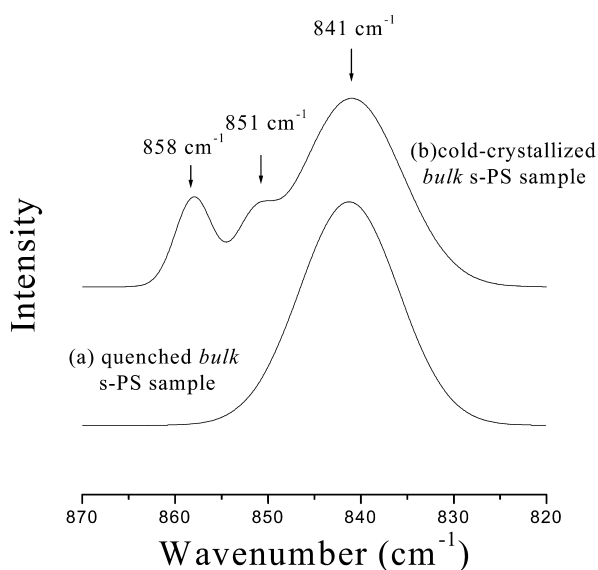


Fig. 5. FTIR spectra of the bulk s-PS sample ranging from 870 to 820  $\text{cm}^{-1}$  (5a) quenched sample; (5b) under melt-crystallization for 2 min.

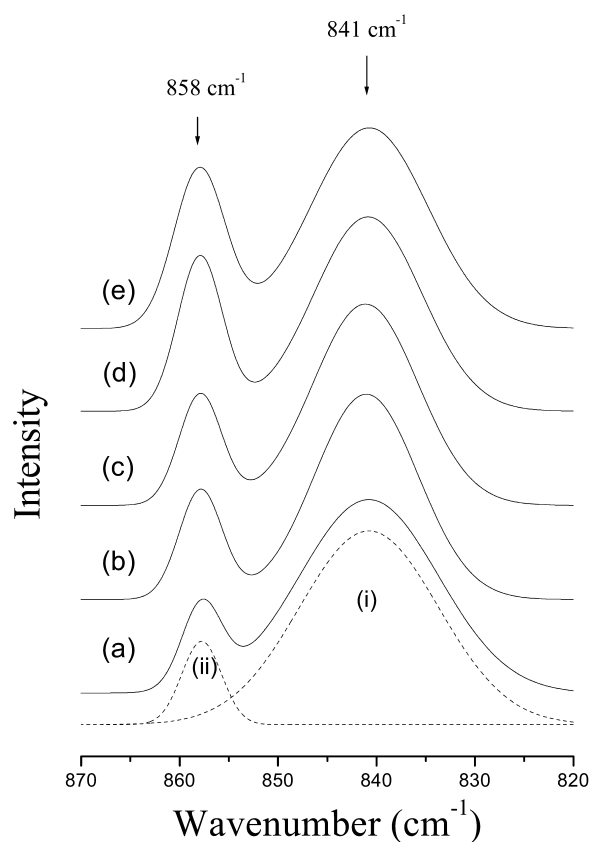


Fig. 6. FTIR spectra of the bulk s-PS sample ranging from 870 to 820  $\text{cm}^{-1}$  under melt-crystallization for (6a) 2 min; (6b) 5 min; (6c) 10 min, (6d) 15 min, and (6e) 30 min. (dash line of 6(i) and (ii) represents the result of Fig. 6a curve fitting).

when the time interval is over 10 min. No massive difference is observed, when time interval is increased to 30 min. Therefore, a bulk s-PS sample that contains absolute  $\beta$ -form crystallinity of over  $\sim 0.55$  at 264  $^{\circ}\text{C}$  for 10 min throughout the melt-crystallization.

Table 2

Curve fitting of the range 870–820  $\text{cm}^{-1}$  of s-PS spectra under melt-crystallization process at 264  $^{\circ}\text{C}$

Isothermal time (min)	Curve fitting			Crystallinity	
	Area	Freq. ( $\text{cm}^{-1}$ )	Width ( $\text{cm}^{-1}$ )	$\alpha$ -Form	$\beta$ -Form
2	0.546	840.8	14.1	$\sim 0$	0.31
	0.067	857.8	3.9		
5	0.327	841.0	10.5	$\sim 0$	0.45
	0.073	857.9	4.3		
10	0.357	841.1	10.6	$\sim 0$	0.46
	0.080	857.9	4.2		
15	0.958	840.7	11.9	$\sim 0$	0.56
	0.328	858.0	5.1		
30	0.673	841.1	11.0	$\sim 0$	0.56
	0.226	857.9	4.6		

### 3.5. Characterization of cold-crystallization

FTIR spectra of cold-crystallization were obtained in Fig. 7 to compare the DSC trace result in Fig. 2. Fig. 7a–e displays the FTIR spectra of the bulk s-PS sample ranging from 870 to 820  $\text{cm}^{-1}$  under cold-crystallization process following 5, 10, 15, 30 and 60 min interval, respectively. The dashed lines of Fig. 7(i)–(iii) are the results of curve fitting to Fig. 7a as an example. The curve-fitting analysis of the FTIR spectral feature of Fig. 7a–d reveals the presence of three distinct components— $\alpha$ -form absorbances (851  $\text{cm}^{-1}$ ),  $\beta$ -form absorbances (858  $\text{cm}^{-1}$ ) and amorphous absorbances (841  $\text{cm}^{-1}$ ). The results of curve-fitting and crystallinity calculated using Eqs. (1) and (2) are shown in Table 3. The s-PS crystallizes to both  $\alpha$  and  $\beta$ -forms during the cold-crystallization consistent with the well-known DSC trace results, in which two endothermic peaks that correspond to the  $\alpha$  and  $\beta$ -forms in the DSC trace always appear simultaneously during normal cold-crystallization process as shown in Fig. 2.

As shown in Figs. 7 and 8 and Table 3, the  $\alpha$ -form crystal grows rapidly in the initiation stage of cold-crystallization. The crystallinity of the  $\alpha$ -form declines while that of the crystallinity of the  $\beta$ -form increases along during cold-crystallization procedure at 264 °C. The sum of the crystal-

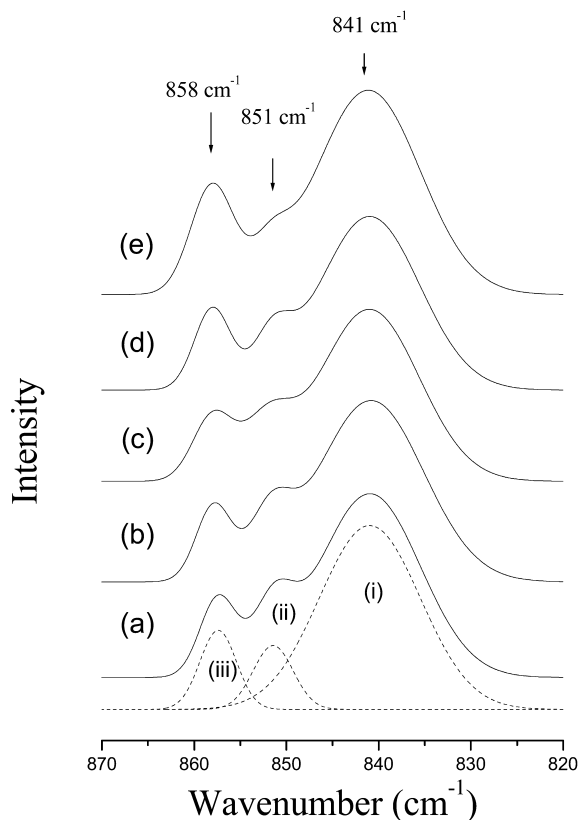


Fig. 7. FTIR spectra of the bulk s-PS sample ranging from 870 to 820  $\text{cm}^{-1}$  under cold-crystallization for (7a) 5 min; (7b) 10 min, (7c) 15 min, (7d) 30 min, (7e) 60 min (dash line of 7(i)–(iii) represents the result of Fig. 7b curve fitting).

Table 3

Curve fitting of the range 870–820  $\text{cm}^{-1}$  of s-PS spectra under cold-crystallization process at 264 °C

Isothermal time (min)	Curve fitting			Crystallinity		
	Area	Freq. ( $\text{cm}^{-1}$ )	Width ( $\text{cm}^{-1}$ )	$\alpha$ -Form	$\beta$ -Form	Total
5	0.576	840.9	11.0			
	0.076	851.7	4.9	0.35		0.52
	0.055	858.1	3.7		0.17	
10	0.576	840.5	9.4			
	0.073	849.0	7.6	0.33		0.53
	0.066	858.2	3.4		0.20	
15	0.306	840.8	9.7			
	0.042	851.4	7.6	0.31		0.56
	0.053	858.1	3.5		0.26	
30	0.617	841.0	10.8			
	0.064	851.5	4.0	0.26		0.55
	0.106	858.0	3.8		0.28	
60	0.476	841.0	10.7			
	0.043	851.5	5.0	0.23		0.55
	0.087	858.0	4.2		0.31	

linities of  $\alpha + \beta$  form is constant ( $\sim 0.55$ ) hence the cold-crystallization proceeds for 10 min interval, implying that no new crystal is transferred from the amorphous phase. It appears that the formation of the  $\beta$ -form is transformed from the  $\alpha$ -form during cold-crystallization in a bulk s-PS sample. It is inferred that the  $\alpha$ -form crystal is kinetically

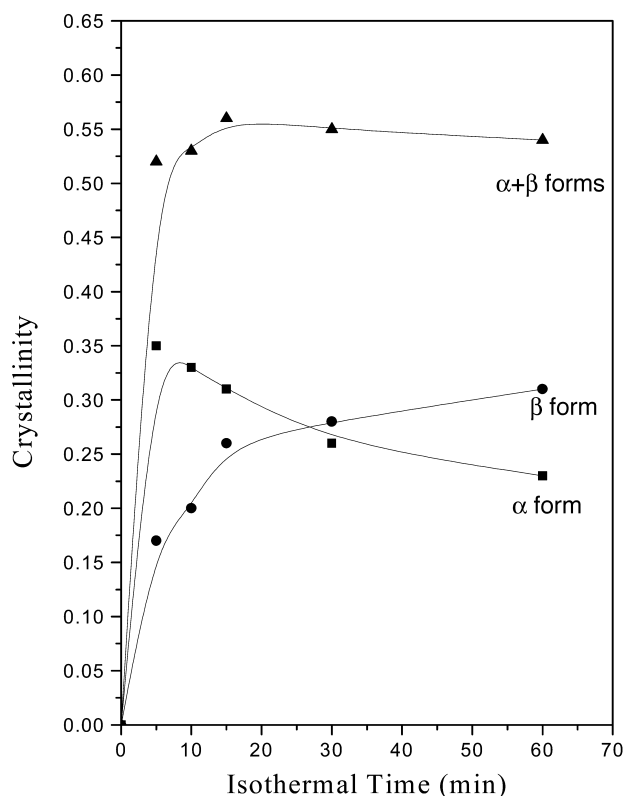


Fig. 8. The crystallinity of  $\alpha$ -form,  $\beta$ -form and  $\alpha + \beta$  form with various isothermal time.

more favorable while the  $\beta$ -form crystal is more thermodynamically favorable based on the obtained FTIR spectra.

Immediate evidence of a crystal phase transformation from the  $\alpha$ -form to the  $\beta$ -form in the bulk s-PS sample cold-crystallization is found in IR spectra. As concluded in our previous study [11–12,14], the cold-crystallized thin film s-PS sample results in an exclusively  $\alpha$ -form crystal. The  $\alpha$  to  $\beta$ -form phase transformation is effectively inhibited in the thin film s-PS sample, but it is permitted in the bulk s-PS sample from the above mentioned immediate evidence.

Comparing Figs. 6–8, and Tables 2 and 3 reveals that the intensity of the  $\alpha$ -form absorbance grows more rapidly higher than that the intensity of  $\beta$ -form absorbance in crystallization, implying that the formation of the  $\alpha$ -form is favored over that of the  $\beta$ -form during crystallization. Apparently, the activity energy of the  $\beta$ -form crystal formation exceeds that of the  $\alpha$ -form.

The asymmetric endothermic peak around  $\sim 270$  and  $260$  °C, implies that a major  $\alpha$ -form and minor  $\beta$ -form crystals are present in the cold-crystallized bulk s-PS sample, respectively, as shown in Fig. 2. Using the traditional DSC tracing, not only does re-crystallization, but also the  $\alpha$  to  $\beta$ -form crystal phase-transformation occurs during the DSC heating scanning in the both cold and melt-crystallized bulk s-PS sample. The re-crystallization in DSC trace makes the observation of s-PS crystallization behavior complication. As a matter of course, it would not provide a quantitative determination of crystallization or (and) kinetics to study bulk s-PS sample. Fortunately, this new FTIR method provides a view to study the above-mentioned topic. It would provide a 'direct' and 'real' quantitative description on the physical property of s-PS bulk sample.

#### 4. Conclusions

This work presents a simple and direct method for detecting the complicated bulk s-PS crystallization behavior. Using FTIR spectra to analyze the bulk s-PS crystallization behavior is able to avoid the interference caused by the re-crystallization and crystal phase transformation by a

typical DSC method. Only the  $\beta$ -form is formed during melt-crystallization, while the both  $\alpha$  and  $\beta$ -forms are presented during cold-crystallization. The formation rate of the  $\alpha$ -form is significantly higher than that of the  $\beta$ -form because formation of  $\alpha$ -form has a lower activation energy. In the cold-crystallization process, the  $\alpha$ -form is formed initially because it is kinetically more favorable. Furthermore, the sum of the crystallinities of  $\alpha + \beta$  is nearly constant ( $\sim 0.55$ ) during cold-crystallization after 5 min. This observation emphasizes that the  $\beta$ -form is produced from the  $\alpha$  form through phase transformation process during cold-crystallization, not directly generated from the amorphous phase. This FTIR method provides immediate and precise evidence of the crystallization behavior of the bulk s-PS sample.

#### Acknowledgements

This financial support of this research was provided by National Science Council, Taiwan, under Contract No. NSC-92-2216-E-009-018.

#### References

- [1] Kellar EJC, Galiotis C, Andrews EH. *Macromolecules* 1996;29:3515.
- [2] Nakaoki T, Kobayashi MJ. *Mol Struct* 1991;242:315.
- [3] Sun YS, Woo EM. *Macromolecules* 1999;32:7836.
- [4] Woo EM, Wu FS. *Macromol Chem Phys* 1998;199:2041.
- [5] Musto P, Tavone S, GrUERRA G, De Rosa C. *J Polym Sci, Part B: Polym Phys* 1997;35:1055.
- [6] Woo EM, Wu FS. *J Polym Sci, Part B: Polym Phys* 1998;36:2725.
- [7] Strobl GR, Hagedorn W. *J Polym Sci, Polym Phys Ed* 1978;16:1181.
- [8] Vittoria V, Ruvolo Filho A, De Candia F. *J Macromol Sci Phys* 1990; B28:411.
- [9] Kellar EJC, Evan AM, Knowles J, Galiotis CL, Andrews EH. *Macromolecules* 1997;30:2400.
- [10] Vittoria V. *Polym Commun* 1990;31:263.
- [11] Wu HD, Wu ID, Chang FC. *Macromolecules* 2000;33:8915.
- [12] Wu HD, Tseng CR, Chang FC. *Macromolecules* 2001;34:2992.
- [13] Ho RM, Lin CP, Tsai HY, Woo EM. *Macromolecules* 2000;33:6517.
- [14] Wu HD, Wu SC, Wu ID, Chang FC. *Polymer* 2001;43:4719.